



# Case Study: Verifying the Safety of an Autonomous Racing Car with a Neural Network Controller

Radoslav Ivanov, Taylor J. Carpenter, James Weimer,  
Rajeev Alur, George J. Pappas, Insup Lee  
University of Pennsylvania  
Philadelphia, Pennsylvania  
{rivanov,carptj,weimerj,alur,pappasg,lee}@seas.upenn.edu

## ABSTRACT

This paper describes a verification case study on an autonomous racing car with a neural network (NN) controller. Although several verification approaches have been recently proposed, they have only been evaluated on low-dimensional systems or systems with constrained environments. To explore the limits of existing approaches, we present a challenging benchmark in which the NN takes raw LiDAR measurements as input and outputs steering for the car. We train a dozen NNs using reinforcement learning (RL) and show that the state of the art in verification can handle systems with around 40 LiDAR rays. Furthermore, we perform real experiments to investigate the benefits and limitations of verification with respect to the *sim2real* gap, i.e., the difference between a system's modeled and real performance. We identify cases, similar to the modeled environment, in which verification is strongly correlated with safe behavior. Finally, we illustrate LiDAR fault patterns that can be used to develop robust and safe RL algorithms.

## CCS CONCEPTS

• **Software and its engineering** → **Formal methods**; • **Computing methodologies** → **Neural networks**; • **Computer systems organization** → **Robotic autonomy**.

## KEYWORDS

Neural Network Verification, Learning for Control, F1/10 Racing

### ACM Reference Format:

Radoslav Ivanov, Taylor J. Carpenter, James Weimer, Rajeev Alur, George J. Pappas, Insup Lee. 2020. Case Study: Verifying the Safety of an Autonomous Racing Car with a Neural Network Controller. In *23rd ACM International Conference on Hybrid Systems: Computation and Control (HSCC '20)*, April 22–24, 2020, Sydney, NSW, Australia. ACM, New York, NY, USA, 7 pages. <https://doi.org/10.1145/3365365.3382216>

This material is based upon work supported by the Air Force Research Laboratory (AFRL) and the Defense Advanced Research Projects Agency (DARPA) under Contract No. FA8750-18-C-0090. Any opinions, findings and conclusions or recommendations expressed in this material are those of the author(s) and do not necessarily reflect the views of the AFRL, DARPA, the Department of Defense, or the United States Government.

Permission to make digital or hard copies of all or part of this work for personal or classroom use is granted without fee provided that copies are not made or distributed for profit or commercial advantage and that copies bear this notice and the full citation on the first page. Copyrights for components of this work owned by others than the author(s) must be honored. Abstracting with credit is permitted. To copy otherwise, or republish, to post on servers or to redistribute to lists, requires prior specific permission and/or a fee. Request permissions from [permissions@acm.org](mailto:permissions@acm.org).

HSCC '20, April 22–24, 2020, Sydney, NSW, Australia

© 2020 Copyright held by the owner/author(s). Publication rights licensed to ACM.  
ACM ISBN 978-1-4503-7018-9/20/04...\$15.00  
<https://doi.org/10.1145/3365365.3382216>

## 1 INTRODUCTION

Neural networks (NNs) have shown great promise in multiple application domains, including safety-critical systems such as autonomous driving [5] and air traffic collision avoidance systems [16]. At the same time, widespread adoption of NN-based autonomous systems is hindered by the fact that NNs often fail in seemingly unpredictable ways: slight perturbations in their inputs can result in drastically different outputs, as is the case with adversarial examples [27]. Such issues might lead to fatal outcomes in safety-critical systems [4] and thus underscore the need to assure the safety of NN-based systems before they can be deployed at scale.

One way to reason about such systems is to formally verify safety properties of a NN's outputs for certain sensitive inputs, as proposed in several NN verification and robustness works [10, 11, 17, 29, 30]. However, safety of the NN does not immediately imply safety of the entire autonomous system. A more exhaustive approach is to consider the interaction between the NN and the physical plant (e.g., a car), trace the evolution of the plant's states (e.g., position, velocity) and ensure all reachable states are safe. A few such methods were developed to verify safety of autonomous systems with NN controllers [9, 15, 26, 28]. These techniques combine ideas from classical dynamical system reachability [7, 18, 28] (e.g., view the NN as a hybrid system) with NN verification approaches (e.g., transform the NN into a mixed integer linear program). However, these approaches have so far been evaluated on fairly simple systems: either systems with low-dimensional NN inputs (i.e., the plant states such as position and velocity [9, 15, 28]) or with constrained environments (e.g., LiDAR orientation does not change over time [26]).

Two main challenges remain in verifying realistic systems. The first one is scalability, with respect to (w.r.t.) both plant dynamics and NN complexity. Since reachability is undecidable for general hybrid systems [3], existing approaches can only approximate the reachable sets. The NN adds complexity not only due to size but also due to the number of inputs to the NN – it is much more challenging to compute reachable sets for multivariate functions, even for small NNs. Having the capability to verify high-dimensional systems is crucial, however, since NNs are most useful exactly in such settings.

The second verification challenge is the *sim2real* gap, i.e., the difference between a system's modeled and real performance [6]. Analyzing the *sim2real* gap is essential as it allows us to explore the benefit of verification w.r.t. the real system. Overcoming this challenge would enable developers to design and test approaches in simulation with the assurance that safety properties that hold in simulation would carry over to the real world.

In order to illustrate these difficulties and to provide a challenging benchmark for future work, this paper presents a verification

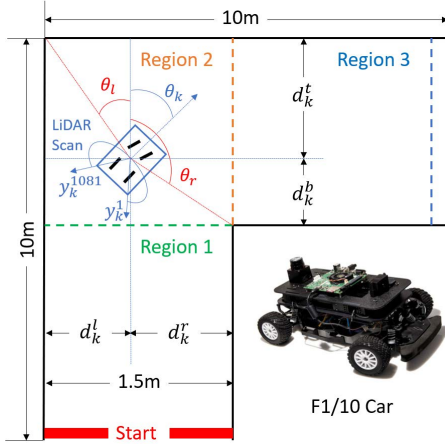


**Figure 1: Navigation scenario. There are three regions depending on how many walls can be reached by LiDAR.**

case study on a realistic NN-controlled autonomous system. In particular, we focus on the F1/10 autonomous racing car [1], which needs to navigate a structured environment using high-dimensional LiDAR measurements. This case study has two goals: 1) assess the capabilities of existing verification approaches and highlight aspects that require future work; 2) investigate conditions under which the verification translates to safe performance in the real world.

To perform the verification, we first identify a dynamics model of the car, as well as an observation model mapping the car state to the LiDAR measurements. To obtain the observation model, we assume the car operates in a structured environment (i.e., a sequence of hallways) such that each LiDAR ray can be calculated based on the car’s state and the surrounding walls. Given these models, we train an end-to-end NN controller using reinforcement learning (RL) [20]. The NN takes LiDAR measurements as input and produces steering as output (assuming constant throttle). Once the NN is trained, we aim to verify that the car does not crash in the hallway walls.

We evaluate the scalability of existing verification tools by varying the NN size, the number of LiDAR rays as well as the training algorithm. Note that the complexity of verification grows exponentially with the number of rays since, depending on the uncertainty, a ray could reach different walls, which correspond to different paths in the hybrid observation model – all such paths need to be verified simultaneously. We use the state-of-the-art tool Verisig [15] to verify the dozen setups that were trained; we could not encode the LiDAR model in the other existing tools. In our evaluation, Verisig could handle NNs containing two layers with 128 neurons each and LiDAR scans with around 40 rays. This highlights the challenge presented by this case study: verifying a full LiDAR scan with 1081 rays, together with a corresponding NN that can process such a scan, remains beyond the capabilities of existing tools.

Finally, we perform experiments, using the verified controllers, to evaluate the system’s sim2real gap. This gap is especially pronounced with LiDAR, since laser rays could provide an erroneous distance if they are reflected. We first perform experiments in an ideal setting with all reflective surfaces covered – all NNs performed similarly in this setup, resulting in safe behavior roughly 90% of the time, where the crashes were still caused by LiDAR faults that

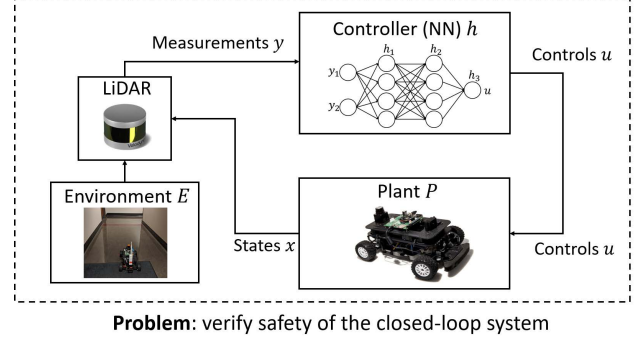


**Figure 2: Overview of the closed-loop system and the problem considered in this paper.**

could not be completely eliminated. More crashes were observed in the unmodified environment, as caused by consistently bad LiDAR data. Interestingly, we identified patterns of LiDAR faults that reproduce the unsafe behavior in simulations as well – however, training (and verifying) a robust controller is left for future work, since state-of-the-art RL algorithms cannot easily handle these faults.

This paper has three contributions: 1) a challenging benchmark for verification and RL in NN-controlled autonomous systems with high-dimensional measurements; 2) an exhaustive evaluation of a state-of-the-art verification tool; 3) real experiments that illustrate the benefits and limitations of verification w.r.t. the sim2real gap.

## 2 SYSTEM OVERVIEW

This section summarizes the different parts of the F1/10 case study. We first describe the F1/10 platform, followed by a high-level introduction to reinforcement learning and hybrid system verification.

### 2.1 The F1/10 Autonomous Racing Car

The case study considered in this paper is inspired by the F1/10 Autonomous Racing Competition [1], where an autonomous car must navigate a structured environment (i.e., the track) as fast as possible. The F1/10 car is shown in Figure 1. It is built for racing purposes and can reach up to 40mph. The car is controlled by an onboard chip such as the NVIDIA Jetson TX2 module.

A diagram of the closed-loop system is shown in Figure 2. The car operates in a hallway environment; without loss of generality, we assume all turns are 90-degree right turns such that the “track” is a square. Although in the competition the car has access to a number of sensors, in this case study the controller only has access to LiDAR measurements. The measurements are sent to a NN controller that outputs a steering command to the vehicle. We assume that the car operates at constant throttle, in order to keep the dynamics model and the verification task manageable. The car’s dynamic and observation models are described in Section 3.

### 2.2 Reinforcement Learning

Overall, developing a robust controller for the F1/10 car is a challenging task, both due to the difficulty of analyzing LiDAR measurements and to the speed and agility of the car. Thus, this is a good application for RL [20], where no knowledge of the car dynamics or the observation model is required. During training, the controller

applies a control action and observes a reward. As training proceeds, the problem is to maximize the reward by exploring the state space and trying different controls. In recent years, deep RL (where controllers are NNs) has shown great promise in a number of traditionally challenging problems, such as playing Atari games [21], controlling autonomous cars [5] and playing board games [25]. Hence, RL is a natural choice for learning a controller for the F1/10 car as well; the specific training approach is described in Section 4.

### 2.3 Hybrid System and NN Verification

At a high level, the hybrid system verification problem is as follows: given a hybrid model of the plant dynamics and observations, the problem is to compute the set of reachable plant states over time (for a set of initial conditions) and verify that no unsafe states can be reached. Although hybrid system reachability is undecidable except for linear systems [3, 19] (see [2, 8] for a discussion), several approaches work well for specific non-linear systems. In particular, reachability is  $\delta$ -decidable for Type 2 computable functions [18], which has led to the development of the tool dReach. Alternatively, Flow\* [7] constructs Taylor model (TM) approximations of the reachable sets. While Flow\* provides no decidability claims, it can verify interesting properties for multiple non-linear systems classes and scales well when using TMs with interval analysis.

Recently, several approaches were developed for verification of hybrid systems with NNs controllers [9, 15, 26, 28]. As described in Section 1, the NN introduces new challenges both due to its size and complexity. To address this issue, the proposed approaches borrow ideas from classical hybrid system reachability, e.g., transform the NN into a mixed-integer linear program (MILP) [9], a satisfiability modulo theory (SMT) formula [26] or an equivalent hybrid system [15]. Although existing tools have shown promising scalability in terms of the size of the NN, they have only been evaluated on low-dimensional systems or systems with constrained environments. This paper provides a more challenging scenario, with a high-dimensional hybrid observation model, in order to test the limits of these tools and to highlight avenues for future work.

### 2.4 System Design and Development

In order to build and verify the system, we perform the following steps: 1) model the car dynamics and observations; 2) train a NN on the model using RL; 3) verify that the NN-controlled car is safe w.r.t. the model; 4) perform real experiments to analyze the sim2real gap. The following sections describe each of these steps in more detail.

## 3 PLANT MODEL

This section describes the F1/10 car's dynamical and observation models. These models are used to train the NN controller (Section 4) and to perform the closed-loop system verification (Section 5).

### 3.1 Dynamics model

We use a bicycle model [22, 23] to model the car's dynamics, which is a standard model for cars with front steering. Specifically, we use a kinematic bicycle model since it has few parameters (that are easy to identify) and tracks reasonably well at low speeds, i.e., under 5 m/s [23]. In the kinematic bicycle model, the car has four states: position in two dimensions, linear velocity and heading. The

continuous-time dynamics are given by the following equations:

$$\begin{aligned} \dot{x} &= v \cos(\theta + \beta) \\ \dot{y} &= v \sin(\theta + \beta) \\ \dot{v} &= -c_a v + c_a c_m (u - c_h) \\ \dot{\theta} &= \frac{V \cos(\beta)}{l_f + l_r} \tan(\delta) \\ \beta &= \tan^{-1} \left( \frac{l_r \tan(\delta)}{l_f + l_r} \right), \end{aligned} \quad (1)$$

where  $v$  is the car's linear velocity,  $\theta$  is the car's orientation,  $\beta$  is the car's slip angle and  $x$  and  $y$  are the car's position;  $u$  is the throttle input, and  $\delta$  is the heading input;  $c_a$  is an acceleration constant,  $c_m$  is a car motor constant,  $c_h$  is a hysteresis constant, and  $l_f$  and  $l_r$  are the distances from the car's center of mass to the front and rear, respectively. Since  $\tan^{-1}$  is not supported by most hybrid system verification tools, we assume that  $\beta = 0$ ; this is not a limiting assumption as the slip angle is typically fairly small at low speeds; we did not observe significant differences in the model's predictive power due to this assumption. After performing system identification, we obtained the following parameter values:  $c_a = 1.633$ ,  $c_m = 0.2$ ,  $c_h = 4$ ,  $l_f = 0.225m$ ,  $l_r = 0.225m$ . Finally, we assume a constant throttle  $u = 16$  (resulting in a top speed of roughly 2.4 m/s), i.e., the controller only controls heading. We emphasize that the plant model is fairly non-linear, thus making it difficult to compute reachable sets for the car's states.

### 3.2 Observation model

The F1/10 car has access to LiDAR measurements only. As shown in Figure 1, a typical LiDAR scan consists of a number of rays emanating from -135 to 135 degrees relative to the car's heading. For each ray, the car receives the distance to the first obstacle the ray hits; if there are no obstacles within the LiDAR range, the car receives the maximum range. In this case study, we consider a LiDAR scan with a maximum of 1081 rays and a range of 5 meters.<sup>1</sup>

As shown in Figure 1, there are three regions the car can be in, depending on how many walls can be reached using LiDAR. We present the measurement model for Region 2 only since the other regions are special cases of Region 2. Let  $\alpha_1, \dots, \alpha_{1081}$  denote the relative angles for each ray with respect to the car's heading, i.e.,  $\alpha_1 = -135, \alpha_2 = -134.75, \dots, \alpha_{1081} = 135$ . One can determine which wall each LiDAR ray hits by comparing the  $\alpha_i$  for that ray with the relative angles to the two corners of that turn,  $\theta_l$  and  $\theta_r$  in Figure 1. The measurement model for Region 2 (for a right turn) is presented below, for  $i \in \{1, \dots, 1081\}$ :

$$y_k^i = \begin{cases} d_k^r / \cos(90 + \theta_k + \alpha_i) & \text{if } \theta_k + \alpha_i \leq \theta_r \\ d_k^b / \cos(180 + \theta_k + \alpha_i) & \text{if } \theta_r < \theta_k + \alpha_i \leq -90 \\ d_k^t / \cos(\theta_k + \alpha_i) & \text{if } -90 < \theta_k + \alpha_i \leq \theta_l \\ d_k^l / \cos(90 - \theta_k - \alpha_i) & \text{if } \theta_l < \theta_k + \alpha_i, \end{cases} \quad (2)$$

where  $k$  is the sampling step (the sampling rate is 10Hz),  $d_k^t, d_k^b, d_k^l, d_k^r$  are distances to the four walls, as illustrated in Figure 1, and can be derived from the car's position  $(x, y)$ . Note that computing reachable sets for the observation model is challenging since if a ray

<sup>1</sup> Although typical LiDARs have a longer range than 5m, we found our unit's measurements to be unreliable beyond 5m.

DRL algorithm	NN setup	# LiDAR rays	Controller index	Initial interval size	NN ver. time (s)	Total ver. time (s)	# paths
DDPG	$64 \times 64$	21	1	0.2cm	355	4126	1.32
DDPG	$64 \times 64$	21	2	0.5cm	437	5652	1.975
DDPG	$64 \times 64$	21	3	DNF			
DDPG	$128 \times 128$	21	1	0.2cm	2929	16758	2.13
DDPG	$128 \times 128$	21	2	0.2cm	2744	16308	1.48
DDPG	$128 \times 128$	21	3	DNF			
TD3	$64 \times 64$	21	1	0.5cm	553	4731	2.2
TD3	$64 \times 64$	21	2	0.5cm	853	8094	2.75
TD3	$64 \times 64$	21	3	0.5cm	724	8641	2.725
TD3	$128 \times 128$	21	1	0.5cm	4336	22994	3.025
TD3	$128 \times 128$	21	2	0.5cm	4059	21173	2.9
TD3	$128 \times 128$	21	3	0.5cm	2689	13573	1.775
TD3	$64 \times 64$	41	1	0.2cm*	634	11915	2.102
TD3	$128 \times 128$	41	1	DNF			
TD3	$64 \times 64$	61	1	DNF			
TD3	$128 \times 128$	61	1	DNF			

**Table 1: Verification evaluation for different NN architectures and number of LiDAR rays. The verification times and the number of paths are averaged over all subsets for each setup. Subset sizes are decreased from 0.5cm to 0.2cm and to 0.1cm, if verification fails. DNF setups were terminated after 10 hours on 0.1cm subsets. The notation  $n \times n$  means the NN has two hidden layers and  $n$  neurons per layer. Two out of 100 instances of the 41-ray setup were killed after 24 hours.**

is almost parallel to a wall, small uncertainty in the car’s heading results in large uncertainty in the distance travelled by that ray, as is evident in the division by cosine in the measurement model.

#### 4 CONTROLLER TRAINING

As mentioned in Section 2, the F1/10 case study is a good application domain for deep reinforcement learning (DRL) due to the high-dimensional measurements as well as the non-trivial control policy that is required. This section discusses the DRL algorithms used in the case study as well as the choice of reward function.

Multiple DRL algorithms have been proposed, depending on the learning setup. For discrete control actions, the standard approach is to use a deep Q-network [21] in order to learn the (Q) function that maps a state and an action to the maximum expected reward over a horizon. In the case of continuous actions, a deep deterministic policy gradient (DDPG) approach [20] was developed that approximates the Q function using a Bellman equation. Notably, DDPG uses two NNs, a critic that learns the Q function and an actor that applies the controls. Once training is finished, the actor is used as the actual controller. Multiple improvements over DDPG have been proposed, especially in terms of training stability, e.g., using normalized advanced functions (NAFs) [14], which are a continuous version of Q functions, or using a twin delayed DDPG (TD3) algorithm [13] that employs two critics for greater stability. Finally, model-based DRL algorithms have also been proposed where the NN architecture is designed so as to learn the plant model [12].

In this paper, we focus on the continuous-action-space algorithms as they fit better the F1/10 car control task. For better evaluation, we train controllers using two different algorithms, namely DDPG and TD3 (we could not train good controllers using the authors’ implementation of the NAF-based approach).<sup>2</sup>

An important consideration in any DRL problem is the choice of reward function. In particular, we are interested in a reward function that not only results in better training but also in “smooth” control policies that are easier to verify. Thus, the reward function consists of two parts: 1) a positive gain for every step that does not result in a crash (to enforce safe control) and 2) a negative gain penalizing higher control inputs (to enforce smooth control):

$$r_k = g_p - g_n \delta_k^2, \quad (3)$$

where  $g_p = 10$ ,  $g_n = 0.05$ . A large negative reward of -100 is received if the car crashes. Note that the negative input gain is not applied in turns in order to avoid a local optimum while training.

Another hyper parameter in the training setup is the NN architecture. Although convolutional NNs are easier to train with high-dimensional inputs, they are harder to verify by existing tools since each convolutional layer needs to be unrolled in a fully connected layer with a large number of neurons. Thus, we only consider fully connected architectures in this case study. Scaling to convolutional NNs is thus an important avenue for future work in NN verification.

#### 5 VERIFICATION EVALUATION

Having described the NN controller training process, we now evaluate the scalability of a state-of-the-art verification tool, Verisig [15]. As mentioned in Section 1, the other existing tools cannot currently handle the hybrid observation model. In the considered scenario, the car starts from a 20cm-wide range in the middle of the hallway (as illustrated in Figure 1) and runs for 7s. This is enough time for the car to reach top speed before the first turn and to get roughly to the middle of the next hallway. The safety property to be verified is that the car is never within 0.3m of either wall.

Verisig focuses on NNs with smooth activations (i.e., sigmoid and tanh) and works by transforming the NN into an equivalent hybrid system. The NN’s hybrid system is composed with the plant’s hybrid system, thereby casting the problem as a hybrid system verification

<sup>2</sup>All training, simulation and verification code is available at [https://github.com/rivapp/autonomous\\_car\\_verification](https://github.com/rivapp/autonomous_car_verification).

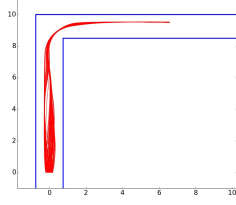
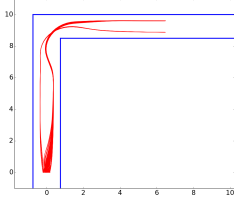
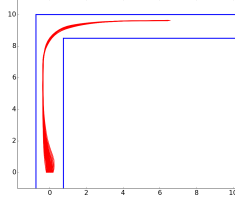
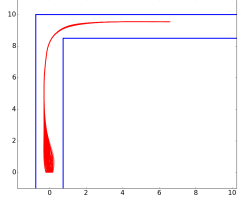
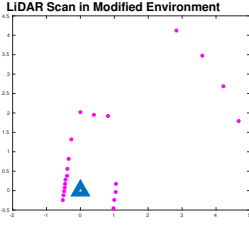
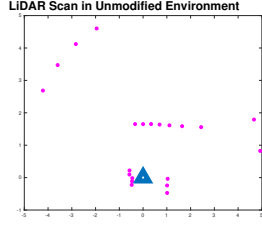
(a) DDPG,  $64 \times 64$ , controller 1.(b) DDPG,  $128 \times 128$ , controller 2.(c) TD3,  $64 \times 64$ , controller 1.(d) TD3,  $128 \times 128$ , controller 1.

Figure 3: Simulation traces for different NN controllers from Table 1.



(a) Modified environment.



(b) Unmodified environment.

Figure 4: LiDAR scans that led to crashes in experiments. Reflected rays appear as if no obstacles exist in that direction.

problem that is solved by Flow\*. In Verisig's original evaluation [15], the tool scales to NNs with about 100 neurons per layer and a dozen layers. The high-dimensional input space considered in this case study, however, presents a greater challenge which might also affect the tool's scalability in terms of the NN size.

All NNs in this case study were trained with tanh activations. The output layer also has a tanh activation, which is scaled by 15 so that the control input ranges from -15 to 15 degrees.<sup>3</sup> As described in Section 4, we use both the DDPG and TD3 algorithms to explore different aspects of the verification process. All NNs have two hidden fully connected layers; the number of neurons per layer is increased from 64 to 128. We also vary the number of LiDAR rays from 21 to 41 and finally to 61 in order to evaluate the scalability in terms of the input dimension as well.<sup>4</sup> For repeatability purposes, we train three controllers for each setup in the 21-ray case.

The verification times<sup>5</sup> for all the setups are presented in Table 1, together with other verification artifacts. Note that the initial interval is split in smaller subsets in order to maintain the approximation error small – the verification is performed separately for each subset. For each setup, only average statistics over all subsets are presented. As can be seen in the table, the biggest setup that Verisig can handle has roughly 40 LiDAR rays. The verification complexity in terms of the number of LiDAR rays is reflected in the last column in the table, which indicates the average number of paths in the hybrid observation model caused by the fact that a LiDAR ray could potentially reach different walls – note that smaller-NN setups can take longer to verify simply due to a higher number of paths since each path needs to be verified separately.

<sup>3</sup>The dynamics model assumes the controls are given in radians – we use degrees in the paper for clearer presentation.

<sup>4</sup>Note that, due to hardware issues with our LiDAR unit, we only used the rays ranging from -115 to 115 degrees (instead of the full scan ranging from -135 to 135 degrees).

<sup>5</sup>All experiments were run on a 80-core machine running at 1.2GHz. However, Flow\* is not parallelized, so the only benefit from the multicore processor is the fact that multiple verification instances can be run at the same time.

A second important observation is that the NN verification time is roughly 10% of the total verification time. This suggests that plant verification remains a greatly challenging problem. Thus, the scalability of verification needs to be greatly improved not only in terms of the NN size but also in terms of the plant complexity.

Finally, the subset size indicates the difficulty of verifying a NN. The subsets were decreased when the safety property could not be verified due to high uncertainty (some NNs could not be verified even with very small subsets). A smaller subset size means a NN is less robust to input perturbations. As an illustration, Figure 3 shows simulation traces for two NNs that either required reducing the subset size or could not be verified at all and for two NNs that were verified with the original subset size of 0.5cm. The first two NNs are very sensitive to their inputs and produce drastically different traces depending on the initial condition. As shown in Section 6, these NNs also result in unsafe behavior in the real world.

## 6 EXPLORING THE SIM2REAL GAP

Having evaluated the scalability of current verification tools, we now investigate the benefits and limitations of verification w.r.t the real system. The sim2real gap arises from imperfect (dynamics and perception) models. While the dynamics model is fairly standard (and worst-case error bounds could be obtained using model validation techniques [24]), the perception model is a major source of uncertainty since surface reflectivity is unknown. Thus, when a ray is reflected, it appears as if no obstacle exists in that direction.

We explore the sim2real gap in an environment that is identical to the verified one in terms of hallway dimensions, the main difference being that the real environment contains reflective surfaces that sometimes greatly affect LiDAR measurements. To assess the quality of the LiDAR model, we first measure its accuracy for non-reflected rays. We collect multiple scans while keeping the car stationary (with a known state) and compare the real data with the model's prediction. We observe that more than 90% of the non-reflected rays are within 5cm of the model's prediction (the bigger errors are likely due to errors in measuring the car's actual orientation).

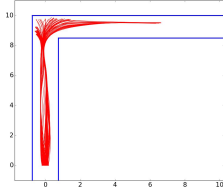
In order to assess the effect of missing rays, we perform experiments in two settings: 1) an ideal environment in which most reflective surfaces are covered and 2) the original unmodified environment.<sup>6</sup> We perform 10 seven-second runs per NN setup in each environment. All outcomes are reported in Table 2. As can be seen in the table, roughly 10% of runs in the modified environment were unsafe, uniformly spread across different NNs, thus indicating

<sup>6</sup>All data traces from the experiments are available at [https://github.com/rivapp/hsc20\\_data\\_traces](https://github.com/rivapp/hsc20_data_traces).

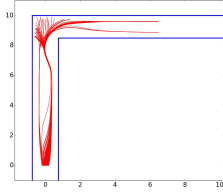


DRL algorithm	NN architecture	# LiDAR rays	Controller Index	Safe outcomes in $Env_M$	Safe outcomes in $Env_U$
DDPG	$64 \times 64$	21	1	9/10	0/10
DDPG	$64 \times 64$	21	2	9/10	2/10
DDPG	$64 \times 64$	21	3	10/10	8/10
DDPG	$128 \times 128$	21	1	10/10	8/10
DDPG	$128 \times 128$	21	2	7/10	4/10
DDPG	$128 \times 128$	21	3	9/10	0/10
TD3	$64 \times 64$	21	1	8/10	9/10
TD3	$64 \times 64$	21	2	10/10	9/10
TD3	$64 \times 64$	21	3	10/10	9/10
TD3	$128 \times 128$	21	1	9/10	9/10
TD3	$128 \times 128$	21	2	9/10	5/10
TD3	$128 \times 128$	21	3	9/10	9/10

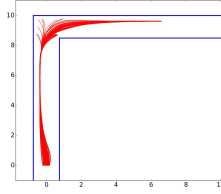
**Table 2: Sim2real gap for the 21-ray setups from Table 1. Ten runs were performed for each setup in both the modified ( $Env_M$ ) and unmodified ( $Env_U$ ) environments. A safe outcome is recorded if the car does not hit a wall during a run.**



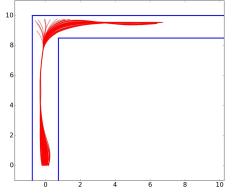
(a) DDPG,  $64 \times 64$ , controller 1: 24% safe.



(b) DDPG,  $128 \times 128$ , controller 2: 51% safe.



(c) TD3,  $64 \times 64$ , controller 1: 75% safe.



(d) TD3,  $128 \times 128$ , controller 1: 83% safe.

**Figure 5: Simulation traces for the NN controllers from Figure 3, with LiDAR faults added around the corner.**

that the LiDAR model is fairly accurate when no reflections occur and that the verification result is strongly correlated with safe performance. We emphasize that LiDAR faults occurred even in this environment – Figure 4a shows a LiDAR scan that caused a crash.

Table 2 also shows that more crashes were observed in the unmodified environment, due to multiple failing LiDAR rays (one scan that led to a crash is shown in Figure 4b). Interestingly, it is possible to produce similar behavior in simulations as well – Figure 5 shows the same runs as those in Figure 3, but with five LiDAR rays randomly missing around the area of the turn, similar to the pattern observed in Figure 4b. The behavior illustrated in Figure 5 is similar to the real outcomes reported in Table 2, e.g., we observe multiple crashes for setups DDPG  $64 \times 64$ , controller 1, and DDPG  $128 \times 128$ , controller 2, while the TD3 NNs are more robust to missing rays.

## 6.1 Robust Reinforcement Learning

Although we can reproduce the LiDAR fault model, training a NN that is robust to such faults was not possible with the DRL algorithms used in the paper. While we did use established sim2real practices (e.g., randomize initial conditions, add measurement noise [6]), the LiDAR fault model presents great robustness challenges since the difference between a reflected and a non-reflected ray could be large. One potential solution is to use a different architecture, e.g., convolutional NNs (CNNs) or recurrent NNs which would add a predictive aspect to the controller.

## 7 DISCUSSION AND FUTURE WORK

This paper presented a challenging verification case study in which an autonomous racing car with a NN controller navigates a structured environment using LiDAR measurements only. We evaluated

a state-of-the-art verification tool, Verisig, on this benchmark and illustrated that current tools can handle only a small fraction of the rays in a typical LiDAR scan. Furthermore, we performed real experiments to assess the benefits of verification in terms of the sim2real gap. Our findings suggest that numerous improvements are necessary in order to address all issues raised by this case study.

*Verification scalability w.r.t. the plant.* As illustrated in Section 5, the verification complexity scales exponentially with the number of LiDAR rays. Thus, it is necessary to develop a scalable approach that addresses this issue. For example, one could use the structure of the environment in order to develop an assume-guarantee approach such that verifying long traces may not be required.

*Verification scalability w.r.t. the NN.* Quantifying scalability w.r.t. the NN is not straightforward since a large, but smooth, NN may be easier to verify than a small, but sensitive, one, as indicated in Table 1. Yet, existing tools need to scale beyond a few hundred neurons in order to handle CNNs, which are much more effective in high-dimensional settings. While there exist tools that can verify properties about convolutional NNs in isolation [29], achieving such scalability in closed-loop systems remains an open problem, partly due to the complexity of the plant model as well.

*Robustness of DRL.* Although DRL has seen great successes in the last few years, it is still a challenge to train safe and robust controllers, especially in high-dimensional problems. As shown in Section 6, LiDAR faults can be reproduced fairly reliably in simulation; yet, we could not train a robust controller using state-of-the-art learning techniques. Thus, it is essential to develop methods that focus on robustness and repeatability, with the final goal of being able to verify the robustness of the resulting controllers.

## REFERENCES

- [1] [n.d.]. F1/10 Autonomous Racing Competition. <http://f1tenth.org>.
- [2] Rajeev Alur. 2011. Formal verification of hybrid systems. In *Embedded Software (EMSOFT), 2011 Proceedings of the International Conference on*. IEEE, 273–278.
- [3] R. Alur, C. Courcoubetis, N. Halbwachs, T. A. Henzinger, P. H. Ho, X. Nicollin, A. Olivero, J. Sifakis, and S. Yovine. 1995. The algorithmic analysis of hybrid systems. *Theoretical computer science* 138, 1 (1995), 3–34.
- [4] US National Transportation Safety Board. [n.d.]. Preliminary Report Highway HWY18MH010. <https://www.ntsb.gov/investigations/AccidentReports/Reports/HWY18MH010-prelim.pdf>.
- [5] Mariusz Bojarski, Davide Del Testa, Daniel Dworakowski, Bernhard Firner, Beat Flepp, Prasoon Goyal, Lawrence D Jackel, Mathew Monfort, Urs Muller, Jiakai Zhang, et al. 2016. End to end learning for self-driving cars. *arXiv preprint arXiv:1604.07316* (2016).
- [6] Yevgen Chebotar, Ankur Handa, Viktor Makoviychuk, Miles Macklin, Jan Issac, Nathan Ratliff, and Dieter Fox. 2019. Closing the sim-to-real loop: Adapting simulation randomization with real world experience. In *2019 International Conference on Robotics and Automation (ICRA)*. IEEE, 8973–8979.
- [7] X. Chen, E. Ábrahám, and S. Sankaranarayanan. 2013. Flow\*: An analyzer for non-linear hybrid systems. In *International Conference on Computer Aided Verification*. Springer, 258–263.
- [8] Laurent Doyen, Goran Frehse, George J Pappas, and André Platzer. 2018. Verification of hybrid systems. In *Handbook of Model Checking*. Springer, 1047–1110.
- [9] Souradeep Dutta, Xin Chen, and Sriram Sankaranarayanan. 2019. Reachability analysis for neural feedback systems using regressive polynomial rule inference. In *Proceedings of the 22nd ACM International Conference on Hybrid Systems: Computation and Control*. ACM, 157–168.
- [10] S. Dutta, S. Jha, S. Sankaranarayanan, and A. Tiwari. 2018. Output Range Analysis for Deep Feedforward Neural Networks. In *NASA Formal Methods Symposium*. Springer, 121–138.
- [11] R. Ehlers. 2017. Formal verification of piece-wise linear feed-forward neural networks. In *International Symposium on Automated Technology for Verification and Analysis*. Springer, 269–286.
- [12] Chelsea Finn and Sergey Levine. 2017. Deep visual foresight for planning robot motion. In *2017 IEEE International Conference on Robotics and Automation (ICRA)*. IEEE, 2786–2793.
- [13] Scott Fujimoto, Herke van Hoof, and David Meger. 2018. Addressing function approximation error in actor-critic methods. *arXiv preprint arXiv:1802.09477* (2018).
- [14] Shixiang Gu, Timothy Lillicrap, Ilya Sutskever, and Sergey Levine. 2016. Continuous deep q-learning with model-based acceleration. In *International Conference on Machine Learning*. 2829–2838.
- [15] Radoslav Ivanov, James Weimer, Rajeev Alur, George J Pappas, and Insup Lee. 2019. Verisig: verifying safety properties of hybrid systems with neural network controllers. In *Proceedings of the 22nd ACM International Conference on Hybrid Systems: Computation and Control*. ACM, 169–178.
- [16] K. D. Julian, J. Lopez, J. S. Brush, M. P. Owen, and M. J. Kochenderfer. 2016. Policy compression for aircraft collision avoidance systems. In *Digital Avionics Systems Conference (DASC), 2016 IEEE/AIAA 35th*. IEEE, 1–10.
- [17] G. Katz, C. Barrett, D. L. Dill, K. Julian, and M. J. Kochenderfer. 2017. Reluplex: An efficient SMT solver for verifying deep neural networks. In *International Conference on Computer Aided Verification*. Springer, 97–117.
- [18] S. Kong, S. Gao, W. Chen, and E. Clarke. 2015. dReach:  $\delta$ -reachability analysis for hybrid systems. In *International Conference on TOOLS and Algorithms for the Construction and Analysis of Systems*. Springer, 200–205.
- [19] G. Lafferriere, G. J. Pappas, and S. Yovine. 1999. A new class of decidable hybrid systems. In *International Workshop on Hybrid Systems: Computation and Control*. 137–151.
- [20] T. P. Lillicrap, J. J. Hunt, A. Pritzel, N. Heess, T. Erez, Y. Tassa, D. Silver, and D. Wierstra. 2015. Continuous control with deep reinforcement learning. *arXiv preprint arXiv:1509.02971* (2015).
- [21] V. Mnih, K. Kavukcuoglu, D. Silver, A. A. Rusu, J. Veness, M. G. Bellemare, A. Graves, M. Riedmiller, A. K. Fidjeland, G. Ostrovski, et al. 2015. Human-level control through deep reinforcement learning. *Nature* 518, 7540 (2015), 529.
- [22] Philip Polack, Florent Althé, Brigitte d’Andréa Novel, and Arnaud de La Fortelle. 2017. The kinematic bicycle model: A consistent model for planning feasible trajectories for autonomous vehicles?. In *Intelligent Vehicles Symposium (IV), 2017 IEEE*. IEEE, 812–818.
- [23] Rajesh Rajamani. 2011. *Vehicle dynamics and control*. Springer Science & Business Media.
- [24] Robert G Sargent. 2010. Verification and validation of simulation models. In *Proceedings of the 2010 winter simulation conference*. IEEE, 166–183.
- [25] D. Silver, A. Huang, C. J. Maddison, A. Guez, et al. 2016. Mastering the game of Go with deep neural networks and tree search. *nature* 529, 7587 (2016), 484.
- [26] Xiaowu Sun, Haitham Khedr, and Yasser Shoukry. 2019. Formal verification of neural network controlled autonomous systems. In *Proceedings of the 22nd ACM International Conference on Hybrid Systems: Computation and Control*. ACM, 147–156.
- [27] C. Szegedy, W. Zaremba, I. Sutskever, J. Bruna, D. Erhan, et al. 2013. Intriguing properties of neural networks. *arXiv preprint arXiv:1312.6199* (2013).
- [28] Hoang-Dung Tran, Feiyang Cai, Manzan Lopez Diego, Patrick Musau, Taylor T Johnson, and Xenofon Koutsoukos. 2019. Safety Verification of Cyber-Physical Systems with Reinforcement Learning Control. *ACM Transactions on Embedded Computing Systems (TECS)* 18, 5s (2019), 105.
- [29] Shiqi Wang, Kexin Pei, Justin Whitehouse, Junfeng Yang, and Suman Jana. 2018. Efficient formal safety analysis of neural networks. In *Advances in Neural Information Processing Systems*. 6367–6377.
- [30] Tsui-Wei Weng, Huan Zhang, Hongge Chen, Zhao Song, Cho-Jui Hsieh, Luca Daniel, Duane Boning, and Inderjit Dhillon. 2018. Towards Fast Computation of Certified Robustness for ReLU Networks. In *International Conference on Machine Learning*. 5273–5282.